Springer

KSME

Journal of Mechanical Science and Technology 31 (12) (2017) 5705~5710
www.springerlink.com/content/1738-494x(Print)/1976-3824(Online)
DOI 10.1007/s12206-017-1111-3

Estimating the mechanical properties of polyurethane-impregnated felt pads[†]

Dasol Lee[1] and Hyunseop Lee[2,*]

[1]*School of Mechanical Engineering, Pusan National University, Busandaehak-ro 63 beon-gil, Geumjeong-gu, Busan 46241, Korea*
[2]*School of Mechanical Engineering, Tongmyong University, Sinseonno, Nam-gu, Busan 48520, Korea*

(Manuscript Received July 14, 2017; Revised August 3, 2017; Accepted August 3, 2017)

Abstract

Chemical mechanical polishing (CMP) is an essential process in semiconductor fabrication. The results of CMP process are determined with the selection of consumables and process parameters. The polishing pad transports the slurry to the interface between the polishing pad and wafer and obtains material removal planarity. The mechanical properties of the polishing pad should be studied to analyze the material removal mechanism of CMP because polishing pad deformation is directly related to material removal rate and its uniformity. Various studies have investigated the stress distribution of the CMP process by using the elastic modulus and Poisson's ratio of the polishing pad. However, these aspects of polishing pad have not been fully elucidated. In this study, we estimated the mechanical properties of commercial polyurethane-impregnated felt pads by comparing the experimentally measured compressive deformation amounts with finite element analysis results.

Keywords: Chemical mechanical polishing (CMP); Elastic modulus; Poisson's ratio; Polishing pad; Polyurethane-impregnated felt pad

---

1. Introduction

Chemical mechanical planarization is a critical step in semiconductor manufacturing [1-3]. The polishing pad is one of the important consumables in polishing and Chemical mechanical polishing (CMP) processes [4]. The polishing pad is attached to the platen, which comprises polyurethane or polyurethane-impregnated felts [5]. The rough surface is constantly regenerated through conditioning between the runs or during the process [6, 7]. The wafer surface is removed by relative motion between the wafer and polishing pad. The polishing pad deformation is directly related to Material removal rate (MRR) and its uniformity [8-10]. Various studies have investigated polishing pad deformation and the stress exerted to the wafer. Most of these studies have assumed that the polishing pad is an elastic material. Thus, the mechanical properties of the polishing pad should be studied to analyze and predict the CMP process.

The polishing pad can be largely classified as either a microporous polymer sheet pad (Hard type; IC series) or felted polymer fiber-impregnated pad (Soft type; SUBA series) according to pad hardness [11]. IC™ and SUBA™ series pads are marketed under the trade name of Dow Chemical Company. Luo and Dornfeld [12] assumed that the polishing pad is a linear elastic material with a 5.2 MPa elastic modulus (E) and 0.5 Poisson's ratio (v) as a commercial IC-1000 pad. Wang et al. [13] and Lee et al. [14] adopted $v = 0.1$ for commercial polishing pads. Lin et al. [15] used $E = 2.2897$ MPa and $v = 0.1$ for sub-pads. According to Zhang [16], the Poisson's ratio of polishing pad can range from 0.1 to 0.4. Generally, a low Poisson's ratio is related to high pad porosity. Table 1 shows the previously studied material properties of polishing pads. Based on the literature, the elastic modulus and Poisson's ratio of polishing pads have not yet been fully elucidated.

Table 1. Previously reported material properties of polishing pads.

Pad type	Reference	E (MPa)	v
N/A	Lin et al. [15]	2.2897	0.1
Soft pad	Wang et al. [13]	0.34	0.1
IC-1000	Luo and Dornfeld [12]	5.2	0.5
IC-1010	Chen et al. [17]	5	0.1
N/A	Ring et al. [18]	200	0.25
SUBA IV	Kim et al. [19]	115	0.2–0.3
IC-1000	Kim et al. [19]	380	0.3–0.4
IC-1000/SUBA IV stacked	Lee et al. [20]	10	0.2

Particularly, polyurethane-impregnated felt pads have been used for substrate manufacturing to obtain the required surface roughness. This type of felt pad is typically adopted in final

---

[*] Corresponding author. Tel.: +82 51 629 1597, Fax.: +82 51 629 1589
E-mail address: hslee@tu.ac.kr
This paper was presented at the ICMDT2017, Ramada Plaza Jeju Hotel, Jeju, Korea, April 19-22, 2017. Recommended by Guest Editor Dong-Gyu Ahn.

Table 2. Thickness and hardness values of polishing pads.

Pads	Thickness (mm)	Hardness (Asker C)
SUBA^{TM} 400	~1.30	60
SUBA^{TM} 600	~1.30	80
SUBA^{TM} 800	~1.30	83

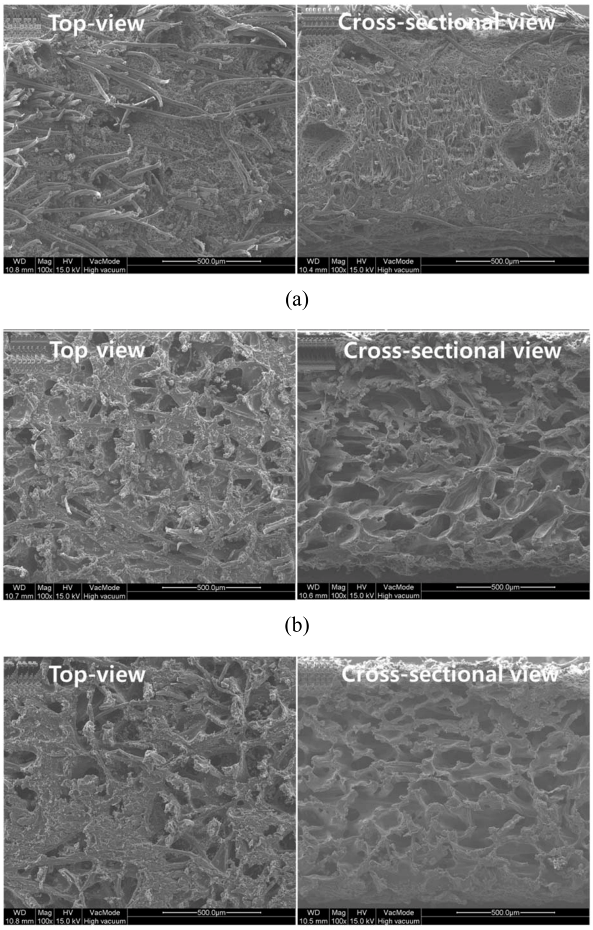

(a)

(b)

(c)

Fig. 1. Scanning electron microscope (SEM) images of polishing pads: (a) SUBA^{TM} 400; (b) SUBA^{TM} 600; (c) SUBA^{TM} 800.

polishing.

In this study, we estimated the mechanical properties of commercial polyurethane-impregnated felt pads by comparing the experimentally measured compressive deformation amounts with Finite element analysis (FEA) results.

2. Experimental conditions

2.1 Felt-typed polishing pad

In this experiment, three types of commercial felt-type polishing pads were prepared to measure the deformation under various loading conditions. Table 2 shows the prepared polishing pads and their thickness and hardness values (Asker C).

The SUBA^{TM} series pads are designed for the polishing of silicon wafer manufacturing. Fig. 1 shows the top and cross-sectional views of polishing pads measured with SEM.

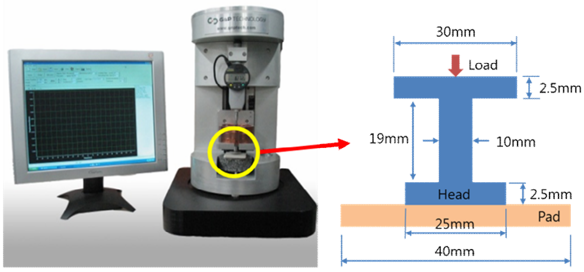

Fig. 2. VMS for deformation testing of polishing pad.

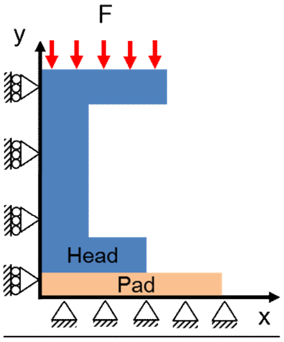

Fig. 3. Schematic of 2D axisymmetric model for FEA.

As shown in Fig. 1, the SUBA^{TM} series is a polyurethane-impregnated pad. The primary difference among the selected polishing pads is the level of polyurethane impregnation. A larger number in the product name indicates a higher level of polyurethane impregnation. On the surface of SUBA^{TM} 400, polyester fibers are present as partial polyurethane impregnation, whereas many pores are present on SUBA^{TM} 800.

2.2 Deformation test

The deformation tests were conducted by using a viscoelasticity measurement system (VMS; G&P Technology). The cycle of loading (1 min) and recovery (1 min) was repeated 90 times. The applied loads were 4.81, 9.63 and 14.44 N for measuring the deformation characteristics of polishing pads under constant pressure. The diameter of circular head was 25 mm, and the sample size of the polishing pad was 40 mm×40 mm. Fig. 2 depicts the VMS and dimensions of the head and pad.

2.3 FEA

We employed FEA to investigate the elastic modulus and Poisson's ratio of the polishing pad. The 2D axisymmetric static model of the simplified VMS system was established, as shown in Fig. 3.

The ranges of the elastic modulus and Poisson's ratio were 0.2–1.2 MPa and 0.1–0.4, respectively. The axisymmetric finite model was constructed using the commercially available

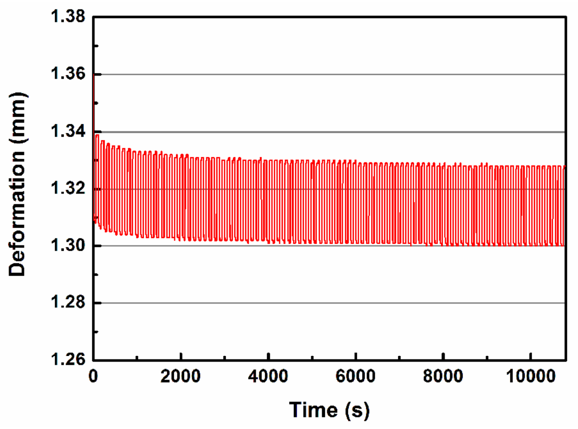

Fig. 4. Pad deformation during 90 cycles of loading–recovery (SUBA 400™ pad).

ANSYS Workbench software.

A quadrilateral mesh was used, and the numbers of nodes and elements were 58283 and 18975, respectively. The pad deformations under various loads, elastic moduli, and Poisson’s ratios were compared with the experimentally measured values.

3. Result and discussion

3.1 Pad deformation

Polishing pad have viscoelastic characteristics because they are typically composed of polyurethane. Polyurethane molecular structures vary from rigid cross-linked polymers to linear, highly extensible elastomers. In the initial stage of a compression test, the polishing pad is significantly compressed, as shown in Fig. 4. Pad deformation is stabilized as loading–recovery cycle continues. The polishing pad has a strain rate depending on time. The polishing pad deformation is stabilized in consecutive CMP processes because pad conditioning and pad break-in processes occur prior to the main polishing step. To estimate the mechanical properties of the polishing pads, we considered a representative loading–re covery cycle after the pad deformation stabilizes.

Figs. 5-7 show the deformation for the three types of pads during the 90th loading–recovery cycle. The applied loads were 4.81, 9.63 and 14.44 N. According to the experimental results, the SUBA™ 400 pad showed the largest deformation among the other polishing pads because it obtained the lowest level of polyurethane impregnation. Polyurethane impregnation influenced the mechanical properties of the polishing pad. As shown in Table 2, the hardness of the polishing pad increases with the increase of polyurethane impregnation. The deformation amounts of SUBA™ 400 under 4.81, 9.63 and 14.44 N were 0.025, 0.044 and 0.064 mm, respectively.

As shown in the figure, the deformation amount decreases with the increase of polyurethane impregnation level. The deformation amounts of SUBA™ 600 under 4.81, 9.63 and 14.44 N were 0.012, 0.024 and 0.038 mm, respectively. The deformation amounts of SUBA™ 800 were 0.009, 0.018 and 0.026 mm with the increase in applied load.

The elastic strain influenced the real contact area between the polishing pad and wafer, which affected the MRR. In addition, the viscoelastic strain affected the wafer non-uniformity because the polishing pad surface became non-uniform before the viscoelastic strain was fully recovered.

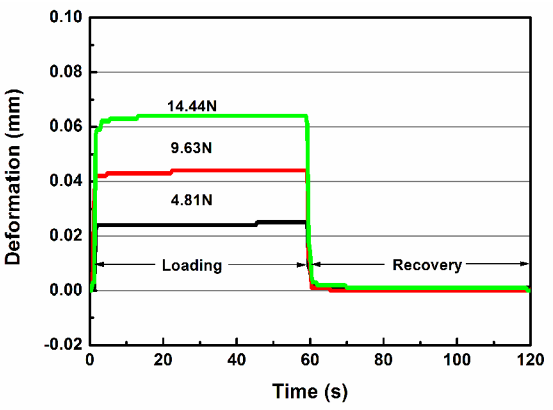

Fig. 5. Deformation of SUBA 400™ pad during the loading–recovery cycle under various loading conditions.

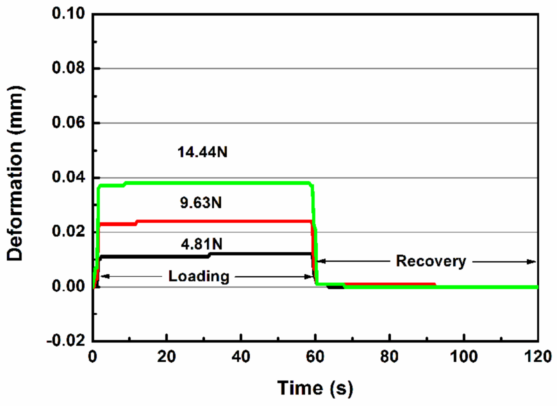

Fig. 6. Deformation of SUBA 600™ pad during the loading–recovery cycle under various loading conditions.

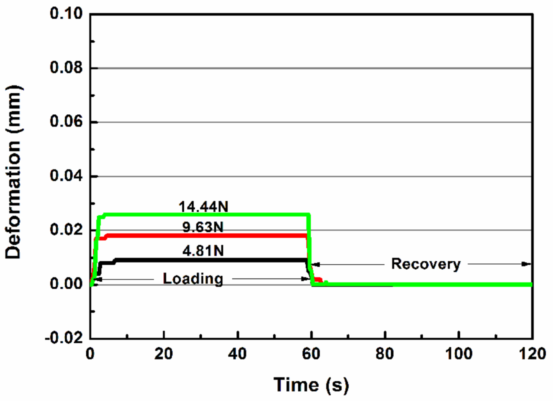

Fig. 7. Deformation of SUBA 800™ pad during the loading–recovery cycle under various loading conditions.

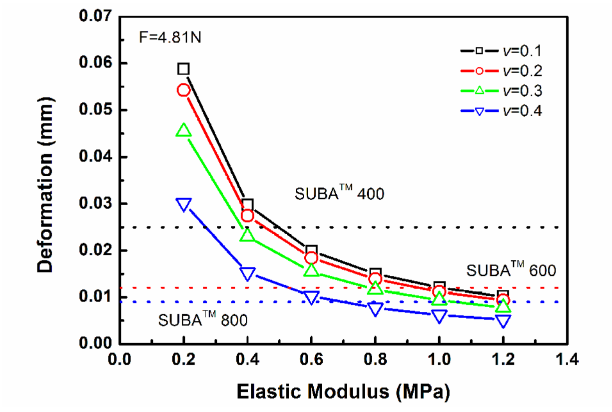

Fig. 8. Simulated pad deformation as a function of elastic modulus and Poisson's ratio under 4.81 N load (Dotted lines are experimentally measured pad deformations).

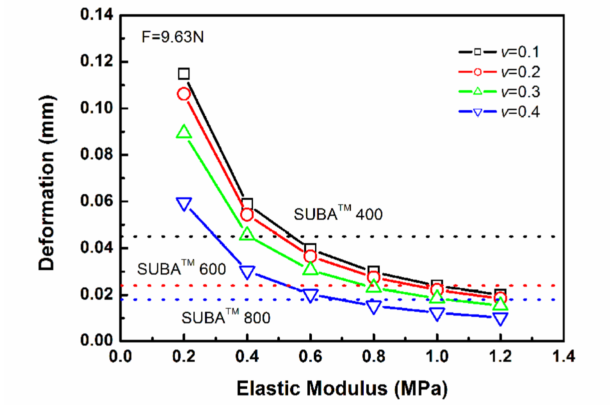

Fig. 9. Simulated pad deformation as a function of elastic modulus and Poisson's ratio under 9.63 N load (Dotted lines are experimentally measured pad deformations).

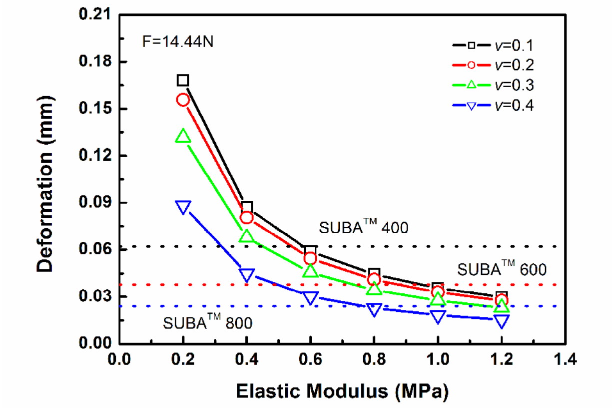

Fig. 10. Simulated pad deformation as a function of elastic modulus and Poisson's ratio under 14.44 N load (Dotted lines are experimentally measured pad deformations).

Table 3. Estimated elastic modulus and Poisson's ratio for the three types of polishing pads.

Pads	Elastic modulus (MPa)	Poisson's ratio
SUBA™ 400	~0.4	~0.3
SUBA™ 600	~0.8	~0.3
SUBA™ 800	~1.0	~0.3

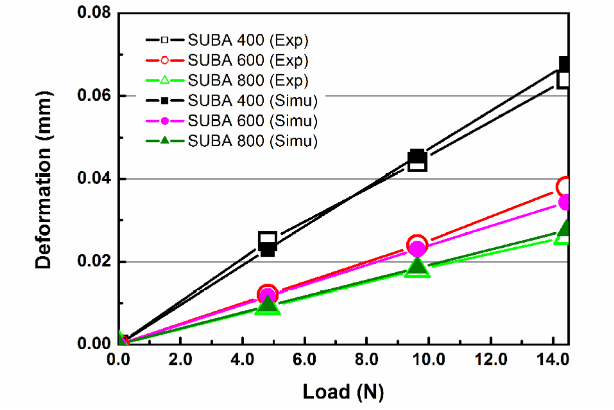

Fig. 11. Simulated and experimental pad deformation as a function of applying load for various polishing pads.

3.2 Estimation of elastic modulus and Poisson's ratio

In this study, we used FEA to estimate the elastic modulus and Poisson's ratio of the polishing pad under various loading conditions. Figs. 8-10 present the simulation results of the pad deformation according to the elastic modulus and Poisson's ratio, which ranged from 0.2—1.2 MPa and 0.1—0.4, respectively. The dotted lines indicate the experimentally measured pad deformations for the three types of polishing pads. The deformation values decreased according to the elastic modulus and Poisson's ratio.

According to Figs. 8-10, the elastic modulus of SUBA™ 400 pad ranged from 0.30 MPa to 0.59 MPa. In Fig. 8, the values of the elastic modulus and Poisson's ratio close to the experimental results of SUBA™ 400 pad were 0.4 MPa and 0.3, respectively. Under 9.63 N and 14.44 N of loads, the same results were obtained, as shown in Figs. 9 and 10.

As shown in the figures, the elastic modulus and Poisson's ratio for SUBA™ 600 pad were approximately 0.8 MPa and 0.3, respectively, whereas approximately 1.0 MPa and 0.3 for SUBA™ 800 pad.

The approximately estimated elastic moduli and Poisson's ratios of the polishing pads are listed in Table 3. Fig. 11 shows the experimentally obtained and simulated deformation amounts of the polishing pads. The simulation results of the proposed approximate elastic moduli and Poisson's ratios agreed with the experimental results.

Fig. 12 shows the simulated pad deformations of the polishing pads as a function of distance from the pad center. The applied pressures for the 6 in wafer and retaining ring are 29.42 kPa and 39.23 kPa. A quadrilateral mesh was used, and the number of nodes and elements were 50214 and 15250.

Fig. 13 illustrates the simulated von-Mises stress distributions of the wafer. As shown in Wang's research [13], the von-Mises stress notably increases near the wafer edge. The polishing pad, which has a lower hardness and elastic modulus

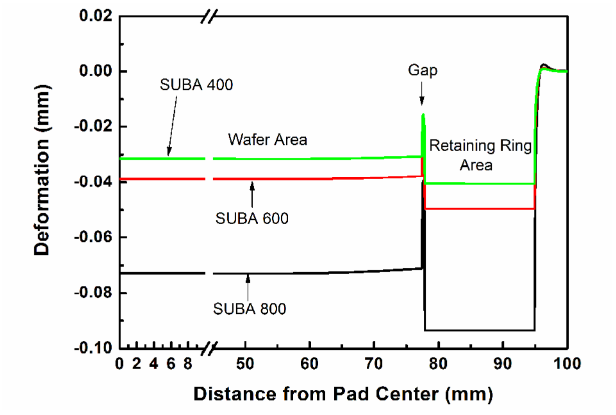

Fig. 12. Simulated pad deformation as a function of distance from pad center: 29.42 kPa for the wafer area; 39.23 kPa for the retaining ring area.

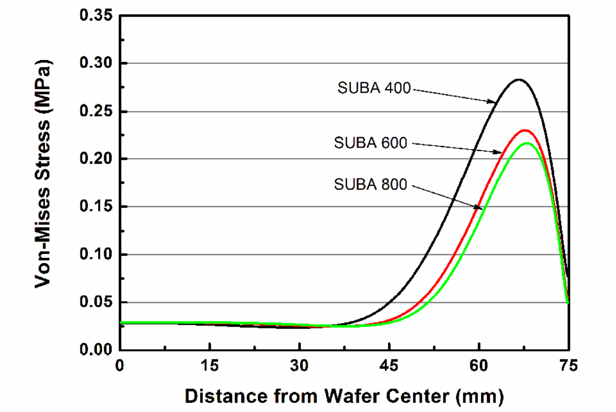

Fig. 13. Simulated von-Mises stress of the wafer as a function of distance from the wafer center: Pressure: 29.42 kPa (Wafer); 39.23 kPa (Retaining ring).

than the other pads, showed a larger value of von-Mises stress near the wafer edge.

4. Conclusions

Polishing performance is sensitive to the mechanical properties of polishing pads. In this study, we examined the elastic modulus and Poisson's ratio of commercial polyurethane-impregnated felt pads by comparing the experimentally measured compressive deformation amounts of FEA results.

For the SEM images, a larger number in the product name indicates a higher level of polyurethane impregnation. The elastic moduli of SUBA^{TM} 400, SUBA^{TM} 600 and SUBA^{TM} 800 were estimated to be approximately 0.4, 0.8 and 1.0 MPa, respectively. Poisson's ratio was approximately 0.3 for the experimental results.

The simulation results of the proposed approximate elastic moduli and Poisson's ratios agreed with the experimental results. In this study, the addressed material properties can be used for analyzing the CMP mechanism and simulating the CMP process.

Acknowledgment

This research was partially supported by the Basic Science Research Program through the National Research Foundation of Korea (NRF) funded by the Ministry of Education (NRF-2015R1D1A1A01059266) and was partially supported by Korea Evaluation Institute of Industrial Technology (10052882).

References

[1] D. Lee, H. Lee and H. Jeong, The effects of a spray slurry nozzle on copper CMP for reduction in slurry consumption, *J. Mech. Sci. Technol.*, 29 (12) (2015) 5057-5062.

[2] D. Lee, H. Lee and H. Jeong, Slurry components in metal chemical mechanical planarization process: A review, *Int. J. Precis. Eng. Manuf.*, 17 (12) (2016) 1751-1762.

[3] H. Lee, Environmental impact of concentration of slurry components in thick copper CMP, *Int. J. Precis. Eng. Manuf.-Green Tech.*, 4 (1) (2017) 13-18.

[4] H. Lee, Mathematical modeling of material removal rate in roll-type linear CMP (Roll-CMP) process: Effect of polishing pad, *Int. J. Precis. Eng. Manuf.*, 17 (4) (2016) 495-501.

[5] M. Yuh, S. Jang, H. Kim, H. Lee and H. Jeong, Development of green CMP by slurry reduction through controlling platen coolant temperature, *Int. J. Precis. Eng. Manuf.-Green Tech.*, 2 (4) (2015) 339-344.

[6] H. Lee and S. Lee, Investigation of pad wear in CMP with swing-arm conditioning and uniformity of material removal, *Precis. Eng.*, 49 (2017) 85-91.

[7] C. Shin, H. Qin, S. Hong, S. Jeon, A. Kulkarni and T. Kim, Effect of conditioner load on the polishing pad surface during chemical mechanical planarization process, *J. Mech. Sci. Technol.*, 30 (12) (2016) 5659-5665.

[8] C. Park, H. Kim, S. Lee and H. Jeong, The influence of abrasive size on high-pressure chemical mechanical polishing of sapphire wafer, *Int. J. Precis. Eng. Manuf.-Green Tech.*, 2 (2) (2015) 157-162.

[9] C. Lee, J. Park, M. Kinoshita and H. Jeong, Analysis of pressure distribution and verification of pressure signal by changes load and velocity in chemical mechanical polishing, *Int. J. Precis. Eng. Manuf.*, 16 (6) (2015) 1061-1066.

[10] S. Park, H. Lee and H. Jeong, Signal analysis of Cmp process based on ae monitoring system, *Int. J. Precis. Eng. Manuf.-Green Tech.*, 2 (1) (2015) 15-19.

[11] H. Lee, D. Lee and H. Jeong, Mechanical aspects of the chemical mechanical polishing process: A review, *Int. J. Precis. Eng. Manuf.*, 17 (4) (2016) 525-536.

[12] J. Luo and D. A. Dornfeld, *Integrated Modeling of Chemical Mechanical Planarization for Sub-Micron IC Fabrication*, Springer-Verlag Berlin Heidelberg, Germany (2004).

[13] D. Wang, J. Lee, K. Holland, T. Bibby, S. Beaudoin and T. Cale, Von mises stress in chemical - mechanical polishing processes, *J. Electrochem. Soc.*, 144 (3) (1997) 1121-1127.

[14] H. Lee and H. Jeong, A wafer-scale material removal rate profile model for copper chemical mechanical planarization,

Int. J. Mach. Tool Manu., 51 (5) (2011) 395-403.

[15] Y. Y. Lin, S. P. Lo, S. L. Lin and J. T. Chiu, A hybrid model combining simulation and optimization in chemical mechanical polishing process, *J. Mater. Proc. Technol.*, 202 (1) (2008) 156-164.

[16] X. Zhang, Chemical mechanical polishing and grinding of silicon wafers, *Ph.D. Dissertation*, Kansas State University, USA (2007).

[17] K. S. Chen, H. M. Yeh, J. L. Yan and Y. T. Chen, Finite-element analysis on wafer-level CMP contact stress: Reinvestigated issues and the effects of selected process parameters, *Int. J. Adv. Manuf. Technol.*, 42 (11) (2009) 1118-1130.

[18] T. A. Ring, P. Feeney, D. Boldridge, J. Kasthurirangan, S. Li and J. A. Dirksen, Brittle and ductile fracture mechanics analysis of surface damage caused during CMP, *J. Electrochem. Soc.*, 154 (3) (2007) H239-H248.

[19] Y. H. Kim, T. K. Kim, H. J. Lee, J. T. Kong and S. H. Lee, CMP profile simulation using an elastic model based on nonlinear contact analysis, *Proc. of 1997 International Conference on Simulation of Semiconductor Processes and Devices*, Cambridge, MA, USA (1997) 69-72.

[20] H. Lee, Y. Park, S. Lee and H. Jeong, Effect of wafer size on material removal rate and its distribution in chemical mechanical polishing of silicon dioxide film, *J. Mech. Sci. Technol.*, 27 (10) (2013) 2911-2916.

Dasol Lee is a Ph.D. student at the School of Mechanical Engineering, Pusan National University, Busan, Korea. She received her M.S. degree in Mechanical Engineering from Pusan National University. Her research interests include chemical mechanical polishing of electronic materials and manufacturing.

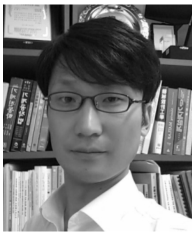

Hyunseop Lee is an Assistant Professor at the School of Mechanical Engineering, Tongmyong University, Busan, Korea. He received his B.S., M.S. and Ph.D. degrees in Mechanical Engineering from Pusan National University. His research fields include chemical mechanical polishing, grinding, and abrasive fluidized bed machining.